JOURNAL OF THERMOPHYSICS AND HEAT TRANSFER
Vol. 12, No. 4, October–December 1998

Technical Notes

TECHNICAL NOTES are short manuscripts describing new developments or important results of a preliminary nature. These Notes cannot exceed 6 manuscript pages and 3 figures; a page of text may be substituted for a figure and vice versa. After informal review by the editors, they may be published within a few months of the date of receipt. Style requirements are the same as for regular contributions (see inside back cover).

Radiative Heat Transfer in a Body-Fitted Axisymmetric Cylindrical Enclosure

Man Young Kim* and Seung Wook Baek†
Korea Advanced Institute of Science and Technology, Taejon 305-701, Republic of Korea

Nomenclature

$\hat{e}_r$, $\hat{e}_z$ = unit vectors in r and z directions, respectively
I^{mn} = directional radiative intensity, W/m^2 sr
$\hat{n}_i$ = unit normal vector at surface i, $n_{i,r}\hat{e}_r + n_{i,z}\hat{e}_z$
$\hat{r}$ = position vector
$\hat{s}$ = unit direction vector, $\sin\theta\cos\phi\,\hat{e}_r + \sin\theta\sin\phi\,\hat{e}_\phi + \cos\theta\,\hat{e}_z$
$\alpha_{mn\pm1/2}$ = coefficients of the angular derivative term, Eq. (6)
ΔA_i, ΔV = surface area and volume of the control volume
θ, ϕ = polar and azimuthal angle measured from $\hat{e}_z$ and $\hat{e}_r$, respectively
κ_a = absorption coefficient, m^{-1}
σ = Stefan-Boltzmann constant, 5.67×10^{-8} W/m^{2}K^4
σ_s = scattering coefficient, m^{-1}
Φ = scattering phase function

Subscripts
E, W, T, B = east, west, top, and bottom neighbors nodal points of P
e, w, t, b = east, west, top, and bottom control volume faces
P = nodal point in which intensities are located
w = wall

Superscripts
mn, $m'n'$ = radiation direction

Introduction

FOR many engineering applications in thermal science, an axisymmetric assumption is usually made to simplify the problem as well as to reduce the computational efforts. For example, the high-temperature flow in a diffuser or converging and diverging nozzle with a variable area as well as in a pipe or can-type gas-turbine combustor having a constant cross-sectional area often allow an axisymmetric assumption. Because these problems occasionally involve a thermal radiation, the solution method treating the thermal radiation in a general body-fitted axisymmetric cylindrical geometry is in high demand.

Received Sept. 3, 1997; revision received March 18, 1998; accepted for publication April 27, 1998.

*Graduate Student, Department of Aerospace Engineering.
†Professor, Department of Aerospace Engineering. E-mail: swbaek@sorak.kaist.ac.kr. Senior Member AIAA.

During the past few decades numerous methods have been proposed to solve the radiative transfer equation (RTE) in the axisymmetric geometry. The S_N discrete-ordinates method (DOM)[1,2] has been widely used, owing to its simple solution procedure, reasonably small computation time, its compatibility with other finite-differenced transport equations, and remarkable solution accuracy. This method, however, has not yet been extended to axisymmetric geometry with curved bounding walls such as in the diffuser or converging and expanding enclosure-like nozzle. For the analysis of axisymmetric radiation, the recently proposed finite volume method (FVM),[3] which is devised with the concept of treating the nonorthogonal geometry, adopts a mapping[4] that yields a complete solution by solving an intensity field in a single azimuthal direction in a three-dimensional cylindrical model. Thereafter, while Chui et al.[5] implemented this method for calculating radiation in a pulverized fuel flame, Baek and Kim[6] applied it to radiative heating of a rocket plume base plane caused by searchlight and plume emissions. Although the axisymmetric FVM has an advantage of flexibility in an irregular or curved geometry with arbitrary control angles, the complexity in the three-dimensional solution procedure as well as in the limited spatial mesh system adopting the perpendicular plane at each axial location because of its mapping, prohibits the use of this FVM in attacking general body-fitted axisymmetric applications, where the grid orthogonality at a bounding curved wall is usually required to capture the physical phenomena.

Recently, Baek and Kim[7] proposed a hybrid method of a modified discrete-ordinates method (MDOM) in an axisymmetric cylindrical geometry. In the MDOM, any set of arbitrary control angles can be chosen as usually done in the FVM, while still keeping a simple calculation procedure as in the conventional DOM. In this work, the MDOM is further extended to analyze a problem of radiative heat transfer in the axisymmetric enclosure with curved wall boundary using the body-fitted mesh system. It is actually achieved by implementing adequate geometrical and directional knowledge. In the following, after formulating the discretization equation in a general axisymmetric geometry with a variable cross-sectional area, it is applied to two benchmark problems such as a truncated cone and a nozzle-shaped cylindrical enclosure. Finally, some concluding remarks are presented.

Formulation

MDOM

To derive the discretization equation in a two-dimensional axisymmetric coordinate, it is necessary to resolve the angular derivative term encountered as a result of angular redistribution. This term can be treated as done by Carlson and Lathrop,[1] i.e.,

$$\frac{\partial(\eta_{mn} I^{mn})}{\partial\phi} = \frac{\alpha_{mn+1/2} I^{mn+1/2} - \alpha_{mn-1/2} I^{mn-1/2}}{\Delta\Omega^{mn}} \tag{1}$$

where

$$\Delta\Omega^{mn} = \int_{\phi^{n-}}^{\phi^{n+}} \int_{\theta^{m-}}^{\theta^{m+}} \sin\theta\, d\theta\, d\phi \tag{2}$$

is the discrete control angle that is analogous to angular weight in the conventional DOM, $\eta = \sin\theta \sin\phi$ is the direction cosine, and $\alpha_{mn\pm1/2}$ is the coefficient for the angular derivative term. Here, it is sufficient to consider only $\sum_{m=1}^{M}\sum_{n=1}^{N}\Delta\Omega^{mn} = 2\pi$ steradians in a solid angle because of its symmetry.

To obtain the discretization equation, the RTE is integrated over the control volume as well as the control angle by assuming that the magnitude of intensity is constant within a control angle, but allowing its direction to vary, as done in the FVM.[1,7,8] Then, the following formulation can be obtained:

$$\sum_{i=e,w,t,b} I_i^{mn}\Delta A_i D_{ci}^{mn} - \frac{\Delta V}{r_P}\left(\alpha_{mn+1/2}I_P^{mn+1/2} - \alpha_{mn-1/2}I_P^{mn-1/2}\right) + (\kappa_a + \sigma_s)_P I_P^{mn}\Delta V\Delta\Omega^{mn} = (S_R^{mn})_P\Delta V\Delta\Omega^{mn} \quad (3)$$

where

$$D_{ci}^{mn} = \int_{\phi^{n-}}^{\phi^{n+}}\int_{\theta^{m-}}^{\theta^{m+}} \sin\theta(n_{i,r}\sin\theta\cos\phi + n_{i,z}\cos\theta)\,d\theta\,d\phi \quad (4)$$

$$S_R^{mn} = \kappa_a I_b + \frac{\sigma_s}{4\pi}\sum_{m'=1}^{M}\sum_{n'=1}^{N} I^{m'n'}\Phi_{m'n'\to mn}\Delta\Omega^{m'n'} \quad (5)$$

While Eq. (4) represents the directional weight,[6,7] which is similar to the multiplication of direction cosine by quadrature weight in the conventional DOM,[1,2] Eq. (5) illustrates the source term composed of both medium emission and in-scattering. To determine the $\alpha_{mn\pm1/2}$ term in Eq. (1), a divergenceless flow is considered as in Carlson and Lathrop.[1] Thereby, the following recursive relation for the coefficients $\alpha_{mn\pm1/2}$ can be obtained:

$$\alpha_{mn-1/2} - \alpha_{mn+1/2} = -\frac{r_P}{\Delta V}\sum_{i=e,w,t,b}\Delta A_i D_{ci}^{mn} \quad (6)$$

with the initial condition of $\alpha_{mN+1/2} = 0$. Note that for the case of right cylinder, the right-hand side of Eq. (6) becomes $-D_{cr}^{mn}$, as shown in Baek and Kim.[7]

Among many schemes, the step scheme[6-11] in spatial differencing and the angular flux value of $I^{mn\pm1/2}$ is chosen as follows:

$$I_e^{mn}D_{ce}^{mn} = I_P^{mn}\max(D_{ce}^{mn}, 0) - I_E^{mn}\max(-D_{ce}^{mn}, 0) \quad (7)$$

$$I_P^{mn-1/2} = I_P^{mn} \qquad m = 1, \ldots, M, \quad n = 1, \ldots, N \quad (8)$$

with the condition of $I_P^{mN+1/2} = I_P^{mN}$. Finally, rearranging Eq. (3) for I_P^{mn}, we obtain the following discretization equation:

$$a_P^{mn}I_P^{mn} = a_E^{mn}I_E^{mn} + a_W^{mn}I_W^{mn} + a_T^{mn}I_T^{mn} + a_B^{mn}I_B^{mn} + b_P^{mn} \quad (9)$$

where

$$a_I^{mn} = \max(-\Delta A_i D_{ci}^{mn}, 0) \quad (10)$$

$$a_P^{mn} = \sum_{i=e,w,t,b}\max(\Delta A_i D_{ci}^{mn}, 0) + (\kappa_a + \sigma_s)_P\Delta V\Delta\Omega^{mn} + \frac{\Delta V}{r_P}\alpha_{mn-1/2} \quad (11)$$

$$b_P^{mn} = (S_R^{mn})_P\Delta V\Delta\Omega^{mn} + \frac{\Delta V}{r_P}\alpha_{mn+1/2}I^{mn+1/2} \quad (12)$$

A similar expression is found in the case of right cylindrical enclosure by Baek and Kim.[7]

Supplementary Equations

Because the detailed information about the control angles, boundary conditions, solution procedure, and convergence criterion is well documented in Baek and Kim,[7] it is not repeated here. But it is noted that the information about $\hat{\boldsymbol{n}}_i$, ΔA_i, and ΔV are required for closing the MDOM in general axisymmetric coordinates, which are readily derived from the geometric relations, for example, in the mesh shown in Fig. 1

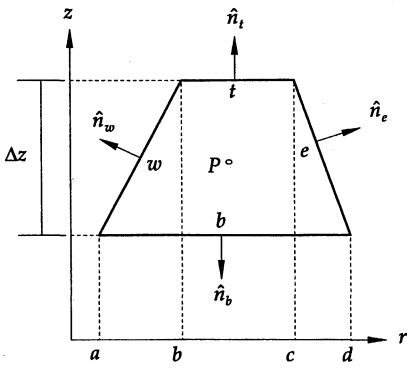

Fig. 1 Cross-sectional side view of a typical control volume.

$$\hat{\boldsymbol{n}}_e = [\Delta z\hat{\boldsymbol{e}}_r + (d-c)\hat{\boldsymbol{e}}_z]/\sqrt{(\Delta z)^2 + (d-c)^2} \quad (13)$$

$$\Delta A_e = \pi(c+d)\sqrt{(\Delta z)^2 + (d-c)^2} \quad (14)$$

$$\Delta V = (\pi/3)\Delta z[(c^2 + cd + d^2) - (a^2 + ab + b^2)] \quad (15)$$

Once the intensity field is calculated, the wall radiative heat flux can be estimated as follows:

$$q_w^R = \int_{\Omega=4\pi} I(\hat{\boldsymbol{r}}_w, \hat{\boldsymbol{s}})(\hat{\boldsymbol{s}}\cdot\hat{\boldsymbol{n}}_w)\,d\Omega = 2\sum_{m=1}^{M}\sum_{n=1}^{N} I_w^{mn}D_{cw}^{mn} \quad (16)$$

where D_{cw}^{mn} is the directional weight at the bounding wall that becomes positive when the radiative beam leaves the wall.

Results and Discussions

To validate the present formulations for the axisymmetric enclosure with a curved wall, two benchmark problems are examined. For all of the cases presented next, a total solid angle of 2π steradians is divided into $(M \times N)$ directions with equal $\Delta\theta = \theta^{m+} - \theta^{m-} = \pi/M$ and $\Delta\phi = \phi^{n+} - \phi^{n-} = \pi/N$. The control angle overlapped at the curved wall is treated following the approach of Moder et al.,[9] which is known as the "bold approximation." For all of the cases studied next, the net radiative heat flux distribution at the bounding side wall of the axisymmetric enclosure is to be calculated.

The first benchmark problem deals with a truncated cone or diffuser-shaped axisymmetric enclosure as depicted in Fig. 2. The side wall is inclined at $\tan^{-1}[(r_2 - r_1)/z_c]$ deg with respect to the z axis, where $r_1 = 0.0833$ m, $r_2 = 0.5833$ m, and $z_c = 1$ m are adopted to compare the result with that of Kaminski,[10] who examined radiative transfer in a conical enclosure using the Monte Carlo and the P_1 approximations. All bounding walls are cold and black, whereas the enclosed medium is hot and has three absorption coefficients of 0.1035, 0.207, and 1.035 m^{-1}. The spatial and angular grid systems of $(N_r \times N_z) = (12 \times 24)$ and $(N_\theta \times N_\phi) = (12 \times 8)$ are used to examine the problem. Denser grids did not change the solution accuracy significantly. Figure 2 shows the nondimensional heat flux distribution along the side wall. In this figure, the present solutions are compared with the Monte Carlo and P_1 solutions. The maximum difference between the present and the Monte Carlo solution amounts to 2.1% near the $z/z_c = 0.5$ for the case of $\kappa_a = 1.035$ m^{-1}.

For the second test problem, the MDOM is applied to a finite axisymmetric cylindrical enclosure with a curved wall like a propulsive nozzle shaped as

$$r/z_c = \tfrac{1}{4}[1 + \sin(\pi z/2z_c)] \quad (17)$$

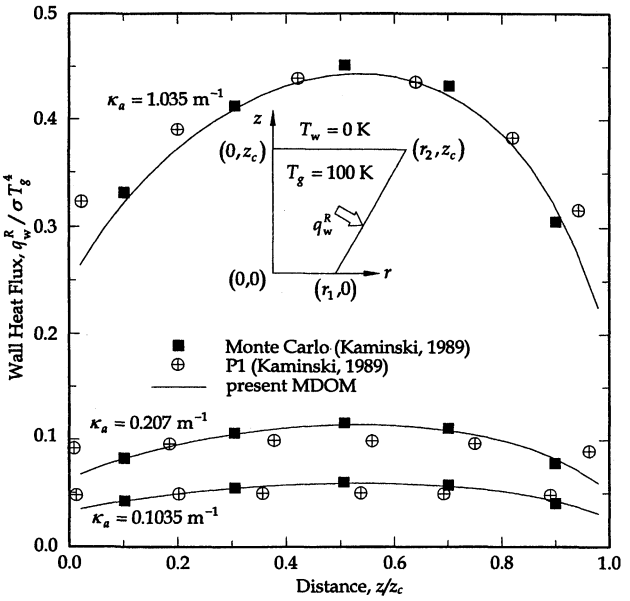

Fig. 2 Comparison of the radiative wall heat flux along the side wall of a truncated cone-shaped enclosure.

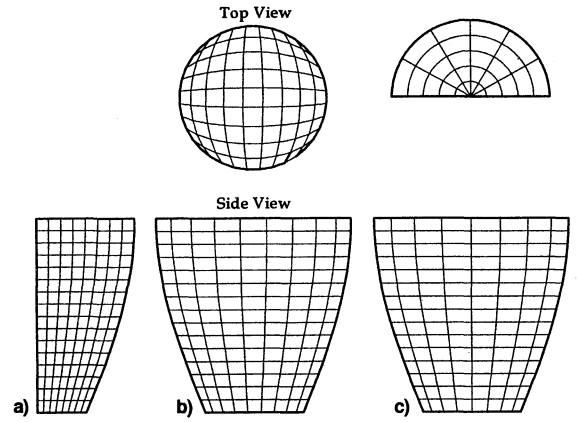

Fig. 3 Top and side views of the spatial grids used in the a) MDOM, b) three-dimensional FVM, and c) axisymmetric FVM.

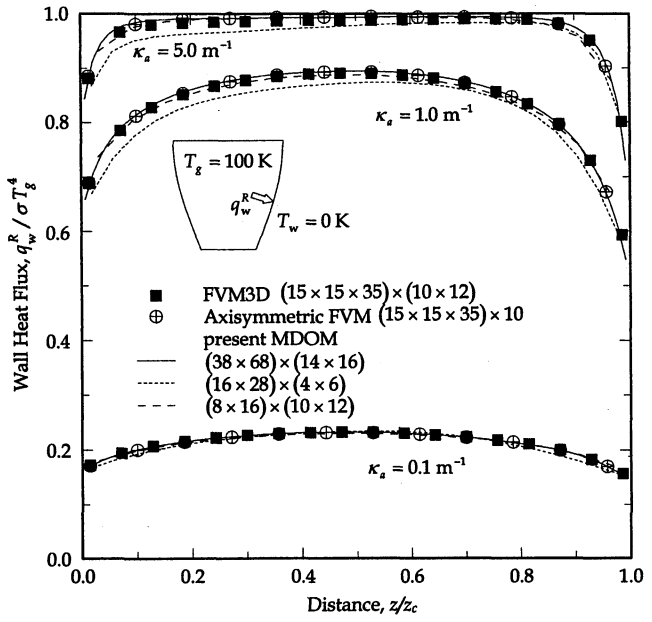

Fig. 4 Comparison of the radiative wall heat flux along the side wall of a nozzle-shaped enclosure.

Table 1 Comparison of the relative average error (%) and computation time (seconds) on a HP 712/75 workstation for a nozzle-shaped cylindrical enclosure[a]

κ_a, m^{-1}	Error, %	Time, s
0.1	2.38[b]/0.54[c]	7.7[b]/41.7[c]
1	3.75/0.84	7.7/41.6
5	2.96/0.49	5.1/32.3

[a]The grid systems of $(N_r \times N_z) \times (N_\theta \times N_\phi) = (16 \times 28) \times (4 \times 6)$ and $(8 \times 16) \times (10 \times 12)$ are used.
[b]$(16 \times 28) \times (4 \times 6)$.
[c]$(8 \times 16) \times (10 \times 12)$

where $z_c = 4$ m is the length of the cylinder. Inside is a hot isothermal medium with three different absorption coefficients of 5, 1, and 0.1 m^{-1}. All of the walls are cold and black. Because there is no benchmark solution to be compared in this case, we have generated other solutions using the nonorthogonal three-dimensional FVM[11] and the axisymmetric FVM.[4,6] Figure 3 represents the spatial grid system used in each solution method. Note that the axisymmetric FVM necessitates a spatially cylindrical three-dimensional mesh shown in Fig. 3c, whereas calculation using the MDOM is performed in a two-dimensional one in Fig. 3a as does the conventional DOM.

Variations of the nondimensional wall heat flux on the side cold wall are plotted in Fig. 4. For $\kappa_a = 5\ m^{-1}$, the radiative heat flux along the side wall is nearly equal to unity because the intensity impinging on the side wall is influenced mainly by the neighboring optically thick hot medium. Near the corners, however, the radiative heat flux sharply decreases because of the top and bottom cold walls. As the absorption coefficient decreases to 0.1 m^{-1}, the heat flux is also reduced because of its reduced emission of the medium and far-reaching effect. In Fig. 4, it is found that the present MDOM yields good results compared with other solutions of the three-dimensional FVM and the axisymmetric FVM. The present MDOM solutions obtained by changing the spatial and angular grid systems are also compared in Fig. 4 and Table 1. Table 1 shows the relative average error and the computation time of the solutions obtained using $(N_r \times N_z) \times (N_\theta \times N_\phi) = (16 \times 28) \times (4 \times 6)$ and $(8 \times 16) \times (10 \times 12)$. Here, the average error means $(q_w^R - q_{w,d}^R)/q_{w,d}^R$ along the side wall divided by N_z, where $q_{w,d}^R$ is the heat flux obtained by using the most fine system of $(38 \times 68) \times (14 \times 16)$. It can be observed that the angular discretization exerts more influence on the heat flux distribution. Overall, the present MDOM yields good results compared with other solutions.

Concluding Remarks

A modified form of the conventional DOM (MDOM) is proposed in a general axisymmetric enclosure with a curved or inclined side wall. The present method is validated by applying it to two benchmark problems of a truncated cone and nozzle-shaped enclosure, and comparing the results with others. All of the results presented in this work supported its solution accuracy in the numerical calculation of axisymmetric radiation. Consequently, the procedure in this study is found to be very useful in analyzing the combined heat transfer in axisymmetric geometry, particularly with a curved shape.

Acknowledgments

The authors are grateful for the financial support by the Korea Science and Engineering Foundation under Contract KOSEF 971-1006-036-2.

References

[1]Carlson, B. G., and Lathrop, K. D., "Transport Theory—The Method of Discrete Ordinates," *Computing Methods in Reactor Physics*, edited by H. Greenspan, C. N. Kelber, and D. Okrent, Gordon

and Breach, New York, 1968, pp. 165–266, Chap. 3.

[2]Fiveland, W. A., "A Discrete-Ordinates Method for Predicting Radiative Heat Transfer in Axisymmetric Enclosure," American Society of Mechanical Engineers, Paper 82-HT-20, 1982.

[3]Raithby, G. D., and Chui, E. H., "A Finite-Volume Method for Predicting a Radiative Heat Transfer in Enclosures with Participating Media," *Journal of Heat Transfer*, Vol. 112, May 1990, pp. 415–423.

[4]Chui, E. H., Raithby, G. D., and Hughes, P. M. J., "Prediction of Radiative Transfer in Cylindrical Enclosures with the Finite-Volume Method," *Journal of Thermophysics and Heat Transfer*, Vol. 6, No. 4, 1992, pp. 605–611.

[5]Chui, E. H., Hughes, P. M. J., and Raithby, G. D., "Implementation of the Finite-Volume Method for Calculating Radiative Transfer in a Pulverized Fuel Flame," *Combustion Science and Technology*, Vol. 92, 1993, pp. 225–242.

[6]Baek, S. W., and Kim, M. Y., "Analysis of Radiative Heating of a Rocket Plume Base with the Finite-Volume Method," *International Journal of Heat and Mass Transfer*, Vol. 40, No. 7, 1997, pp. 1501–1508.

[7]Baek, S. W., and Kim, M. Y., "Modification of the Discrete-Ordinates Method in an Axisymmetric Cylindrical Geometry," *Numerical Heat Transfer, Part B*, Vol. 31, No. 3, 1997, pp. 313–326.

[8]Chai, J. C., Parthasarathy, G., Lee, H. S., and Patankar, S. V., "Finite Volume Radiative Heat Transfer Procedure for Irregular Geometries," *Journal of Thermophysics and Heat Transfer*, Vol. 9, No. 3, 1995, pp. 410–415.

[9]Moder, J. P., Chai, J. C., Parthasarathy, G., Lee, H. S., and Patankar, S. V., "Nonaxisymmetric Radiative Transfer in Cylindrical Enclosures," *Numerical Heat Transfer, Part B*, Vol. 30, 1996, pp. 437–452.

[10]Kaminski, D. A., "Radiative Transfer from a Gray, Absorbing-Emitting, Isothermal Medium in a Conical Enclosure," *Journal of Solar Energy Engineering*, Vol. 111, Nov. 1989, pp. 324–329.

[11]Kim, M. Y., and Baek, S. W., "Prediction of Radiative Heat Transfer in a Three-Dimensional Gas Turbine Combustor with the Finite-Volume Method," *Transactions of the Korean Society of Mechanical Engineers (B)*, Vol. 20, No. 8, 1996, pp. 2681–2692 (in Korean).

Acoustically Levitated Droplet Viscosity Measurement

G. F. Mitchell,* Y. Bayazitoglu,† and R. Shampine‡
Rice University, Houston, Texas 77251-1892

I. Introduction

THE ability to levitate a sample and isolate it from contact with a solid surface prevents the contamination of the sample, which could alter the measured value of the property of interest, and also eliminates surface imperfections that can cause premature solidification in a subcooled liquid sample.[1] While the measurement of surface tension and viscosity are often mentioned together, the theory concerning the containerless measurement of these properties has been seen to diverge somewhat.[2] Chandrasekhar[3] and Reid[4] extended the analysis to permit arbitrary droplet viscosity. These works, however, considered only cases where the viscosity of the host medium surrounding the droplet could be neglected. Miller and Scriven[5] then considered a viscous spherical droplet oscillating in a medium of arbitrary viscosity. More recently, the normal-mode analysis of Prosperetti[6] and the numerical studies of Cumins and Blackburn[7] and Bayazitoglu and Suryanarayana[8–10] have extended the range of theory closer to areas of experimental interest as technological advancements have allowed the measurements of quantities that were once beyond reach.

Earth-based experiments necessarily combine droplet viscosity and static deformation. Nonetheless, containerless surface tension measurements of low-viscosity liquids using Earth-based levitators have obtained good results,[11,12] both in terms of measuring the surface tension and in confirming theoretical predictions for the frequency splitting of deformed droplets.

The viscosity of the droplet serves as a damping force for the oscillations that decay exponentially as $e^{-\beta t}$. Here, β is a complex-valued decay factor, where the real part τ^{-1} is the damping rate and the imaginary part ω corresponds to the natural frequency of oscillations. Theoretical relations between τ, ω, and the viscosity ν exist,[8,13] which allow the viscosity of a liquid to be deduced from the damping rate of droplet oscillations just as natural frequency measurements have been used to find surface tension.

To this point, levitation experiments have focused on properties besides viscosity, which is a much more technically challenging property to measure using levitation. While damping rates have been measured for oscillating viscous droplets suspended in an immiscible liquid of comparable viscosity,[14] such data for liquid droplets oscillating in air have not appeared in the literature.[1] Trinh et al.[14] found discrepancies between the measured and theoretical damping rates that were attributed to the inertia of the viscous boundary layer and temporal variation in the fluid properties near the interface. The present work seeks to obtain damping rate data for liquid-air systems, thereby simplifying the analysis and reducing the inertia of the viscous boundary layer by reducing its thickness. Typical assumptions made for theoretical prediction are isothermal droplets making small-amplitude oscillations about a spherical shape in the absence of external forces and contamination. The present experimental work is intended primarily to test the feasibility of the concepts involved. It should be noted that the droplets are axisymmetric, but not spherical. The levitation forces cause them to be slightly flattened axisymmetrically.

Damping rate information may be obtained through measurement of the decay time or by measuring the sharpness of a resonant peak in the frequency spectrum. Using these methods, three different procedural approaches are possible. The time required for decay could be taken from an oscilloscope trace of the decaying oscillation amplitude immediately following the cessation of the driving force. This approach was used by Trinh et al.[14] in their study of droplets immersed in an immiscible liquid. In their case, however, the natural frequencies were much lower and the liquid host medium provided additional damping.

The damping rate could also be derived from the sharpness or quality factor, Q, of a resonant peak in the response spectrum of the droplet. This could be obtained simply by slowly sweeping the excitation frequency through a natural frequency while measuring the amplitude of the droplet response. This method is also cited by Trinh et al. in their work in immiscible liquid systems. They show the swept frequency response of a silicone/CCl_4 droplet levitated in distilled water, and the resemblance to a bell curve is easily seen. However, it should be noted that a droplet immersed in an immiscible liquid takes on a virtually spherical shape even in gravity caused by the small difference in density between the two liquids. As such, each mode of oscillation exhibits just one resonant peak, in

Received Dec. 23, 1997; revision received May 14, 1998; accepted for publication May 14, 1998.

*Graduate Student; currently Research Engineer, Production Operations Division, Exxon Production Research Company, Houston, TX 77252-2189.

†Professor, Department of Mechanical Engineering and Materials Science, George R. Brown School of Engineering. Member AIAA.

‡Graduate Student; currently Development Engineer, Wellsite Intervention Services, Dowell, Schlumberger, Rosharon, TX 77583-1590.